Molecular Ecology

WILEY

MOLECULAR ECOLOGY

ORIGINAL ARTICLE OPEN ACCESS

The Evolution of Locally Adaptive Chromosome Inversions in *Mimulus guttatus*

Leslie M. Kollar[1,2,3] | Lauren E. Stanley[1,2,3] | Sunil K. Kenchanmane Raju[1,4] | David B. Lowry[1,2,3] | Chad E. Niederhuth[1]

[1]Department of Plant Biology, Michigan State University, East Lansing, Michigan, USA | [2]Plant Resilience Institute, Michigan State University, East Lansing, Michigan, USA | [3]Program in Ecology, Evolution, and Behavior, Michigan State University, East Lansing, Michigan, USA | [4]Department of Botany and Plant Sciences, University of California Riverside, Riverside, California, USA

Correspondence: Leslie M. Kollar (lesliemkollar@gmail.com) | Chad E. Niederhuth (niederhuth@protonmail.com)

Received: 20 August 2024 | **Revised:** 30 January 2025 | **Accepted:** 17 February 2025

Handling Editor: Alison Gonçalves Nazareno

Funding: This study was funded by the National Science Foundation (NSF) Plant Genome Research Program 2010769 to L.M.K. and 2109560 to L.E.S., Michigan State University Plant Biology start-up funds to C.E.N. and by two National Science Foundation Grants to D.B.L. (IOS-1855927 and IOS-2153100).

ABSTRACT

Chromosomal inversion polymorphisms are ubiquitous across the diversity of diploid organisms and play a significant role in the evolution of adaptations in those species. Inversions are thought to operate as supergenes by trapping adaptive alleles at multiple linked loci through the suppression of recombination. While there is now considerable support for the supergene mechanism of inversion evolution, the extent to which inversions trap pre-existing adaptive genetic variation versus accumulate new adaptive variants over time remains unclear. In this study, we report new insights into the evolution of a locally adaptive chromosomal inversion polymorphism (inv_chr8A), which contributes to the adaptive divergence between coastal perennial and inland annual ecotypes of the yellow monkeyflower, *Mimulus guttatus*. This research was enabled by the sequencing, assembly and annotation of new annual and perennial genomes of *M. guttatus* using Oxford Nanopore long-read sequencing technology. In addition to the adaptive inv_chr8A inversion, we identified three other large inversion polymorphisms, including a previously unknown large inversion (inv_chr8B) nested within inv_chr8A. Through population genomic analyses, we determined that the nested inv_chr8B inversion is significantly older than the larger chromosomal inversion in which it resides. We also evaluated the potential role of key candidate genes underlying the phenotypic effects of inv_chr8A. These genes are involved in gibberellin biosynthesis and anthocyanin regulation. Although little evidence was found to suggest that inversion breakpoint mutations drive adaptive phenotypic effects, our findings do support the supergene mechanism of adaptation and suggest it may sometimes involve nested inversions that evolve at different times.

1 | Introduction

Chromosomal inversions have been implicated in evolutionary adaptations since classic studies in *Drosophila* found that inversion polymorphisms are frequently correlated with environmental conditions (Adrion et al. 2015; Dobzhansky 1951, 1970; Hoffmann and Rieseberg 2008; Kapun and Flatt 2019; Kirkpatrick and Kern 2012; Villoutreix et al. 2021). Large chromosomal inversions rearrange the structure of genomes, causing major phenotypic consequences (Dobzhansky 1936; Elgin and Reuter 2013; Lupski 1998; Marshall et al. 2008; Muller 1930; Puig et al. 2015). Inversions strongly suppress

Leslie M. Kollar and Chad E. Niederhuth contributed equally to this work.

genetic recombination in heterokaryotic individuals (inversion heterozygotes) because recombinant gametes are unbalanced (Dobzhansky 1970; Huang and Rieseberg 2020; Rieseberg 2001). Researchers have thus hypothesized that inversions could act as supergenes by holding together haplotype blocks containing multiple locally adaptive polymorphisms through suppressed recombination (Berdan et al. 2023; Dobzhansky 1970; Kirkpatrick and Barrett 2016; Kirkpatrick and Barton 2006; Kirkpatrick and Kern 2012; Darlington and Mather 1950; Schwander et al. 2014; Thompson and Jiggins 2014).

The realisation that inversions could spread rapidly as a result of trapping locally adaptive alleles at linked loci led Kirkpatrick and Barton to ponder nearly two decades ago: 'If the local adaptation mechanism is so powerful, why are inversions not everywhere? One possibility is that they in fact are, and that their frequency has been greatly underestimated' (Kirkpatrick and Barton 2006). Since Kirkpatrick and Barton's (2006) paper, it has become clear that inversion polymorphisms truly are everywhere and are frequently associated with evolutionary adaptations. At least 49 unique inversions have been linked to adaptive phenotypic traits in *Anopheles* mosquitoes (Ayala et al. 2014). Inversions have been shown to control the phenotypes underlying mimicry in butterflies (Joron et al. 2011; Kunte et al. 2014; Thompson and Jiggins 2014) as well as mating and migratory behaviours in birds (Jeong et al. 2022; Lamichhaney et al. 2016; Lundberg et al. 2023; Tuttle et al. 2016). Shifts in the frequency of inversion polymorphisms have been linked to adaptation to forest versus prairie habitats in deer mice (Hager et al. 2022; Harringmeyer and Hoekstra 2022) and to global climate change in *Drosophila* (Anderson et al. 2005; Rane et al. 2015). Inversions appear to play a prominent role in adaptation and domestication of crops, including maize, wheat and peaches (Fang et al. 2012; Pyhäjärvi et al. 2013; Zhang et al. 2015; Zhou et al. 2021). Human and chimpanzee genomes differ by nine major chromosomal inversions and >100 smaller ones (Marquès-Bonet et al. 2004; Newman et al. 2005), which may suggest they played a key role in speciation from our closest relatives (Ayala and Coluzzi 2005; Navarro and Barton 2003). Despite the extensive progress in understanding adaptive inversion evolution, there is still much to learn about how inversions evolve and what genes contribute to their overall phenotypic effects (Berdan et al. 2023).

In this study, we evaluated the evolutionary dynamics of multiple chromosomal inversion polymorphisms in the yellow monkeyflower, *Mimulus guttatus* (syn. *Erythranthe guttata*). This work builds on the previous discovery of a chromosomal inversion polymorphism on chromosome 8 underlying a quantitative trait locus (*DIV1*) in this system. This inversion was originally discovered through controlled crosses and has been shown to be definitively linked to local adaptation through a field reciprocal transplant experiment (Lowry and Willis 2010). While circumstantial evidence has been presented for the role of inversions in local adaptation in many other systems (Beardmore et al. 1960; Butlin and Day 1984; Chouteau et al. 2017; Dobzhansky 1947; Hager et al. 2022; Mérot et al. 2020), this is the only inversion polymorphism that has been definitively linked to local adaptation in the wild (Berdan et al. 2023). The inversion at the *DIV1* locus, which we henceforth refer to as inv_chr8A, has large phenotypic effects on a suite of adaptive traits associated with the transition from an annual to a perennial life history, including flowering time, branching, allocation to vegetative growth and herbivore resistance (Lowry et al. 2019; Lowry and Willis 2010). The inv_chr8A inversion polymorphism is widespread across the geographic range of *Mimulus guttatus*, with one orientation of the inversion commonly found in perennial populations and the other in annual populations (Lowry and Willis 2010). The inversion most strikingly contributes to the divergence of coastal perennial populations, which experience cooler conditions and moisture supplied by summer sea fog, and nearby inland annual populations, which complete their life cycle quickly due to diminishing water availability during summer drought (Hall et al. 2010; Lowry et al. 2008).

Recently, Coughlin and Willis (Coughlan and Willis 2019) provided evidence to support the hypothesis that the inv_chr8A trapped pre-existing adaptive alleles in crosses between annual *M. guttatus* and a perennial sister species, *M. tilingii*, which share the same ancestral chromosomal inversion orientation. The orientation of inv_chr8A found in perennial *M. guttatus* is derived, even though perenniality itself is thought to be the ancestral state in this system (Coughlan and Willis 2019; Friedman 2014). Further, Coughlin and Willis (Coughlan and Willis 2019) were able to exploit free recombination within the inv_chr8A region to show that there are at least two quantitative trait loci (QTL) for morphological divergence in crosses between annual *M. guttatus* and perennial *M. tilingii*. While this result provides some evidence for the supergene hypothesis, how the inversion has evolved over time remains uncertain and the genes underlying the supergene effects of the inversion are still unknown. Identification of the candidate genes that cause the phenotypic effects of inversion polymorphisms in *M. guttatus* has been difficult because available genome assemblies derived from short read sequencing are fragmented (Hellsten et al. 2013) and were available only for ecotypes with the annual orientation. As a result, the full complement of genomic DNA and the inversion breakpoints of the adaptive inv_chr8A and other known inversions have remained unidentified.

Here, we report a set of important new discoveries regarding chromosomal inversion polymorphisms in *M. guttatus*, some of which play crucial roles in the local adaptation and differentiation of annual and perennial ecotypes within this species. This progress was made possible by the sequencing, assembly and annotation of two new genomes for coastal perennial and inland annual lines of *M. guttatus* using Oxford Nanopore technologies that we report here. With these genomes, we were able to overcome previous challenges and identify the breakpoints of these inversions as well as the full complement of genes within the inversions, including inv_chr8A. To identify candidate genes for the adaptive phenotypic effects of the inversions and explore possible phenotypic consequences of the inversion breakpoint mutations themselves, we combined our new genome assemblies with a set of existing population genetic and gene expression datasets. We also combined our analyses with a population genomic data set to evaluate whether particular genes and loci within the adaptive inv_chr8A inversion had undergone recent selective sweeps in either coastal or inland habitats. Through this process, we discovered another large chromosomal inversion (inv_chr8B) nested within inv_chr8A. This finding suggests that this supergene may have begun as a moderate-sized inversion that then expanded by being trapped within a larger inversion. Overall,

this study brings us closer to understanding how chromosomal inversions evolve and why genomes rearrange dramatically over long periods of evolutionary history.

2 | Materials and Methods

2.1 | Tissue Harvesting and DNA Extraction

Our genome sequencing efforts focused on one inland annual line, LMC-L1 (Yorktown, CA, 38°51′50.3388″ N, 123°5′2.1012″ W), and one coastal perennial line, SWB-S1 (Irish Beach, CA, 39°2′9.5388″ N, 123°41′25.6812″ W). While these lines are significant because they have been used in multiple studies (Friedman 2014; Gould et al. 2018; Lowry et al. 2019; Lowry and Willis 2010), we recognise that these lines are not representative of all coastal perennial and inland annuals. LMC-L1 was inbred for 6 generations and SWB-S1 was inbred for 14 generations in the Duke University greenhouses and the Michigan State University growth facilities. The fewer number of generations inbreeding of LMC-L1 is due to the line having a high level of sterility because of inbreeding depression. Floral buds were collected for DNA extractions from plants that were grown in growth chambers in the following conditions: 16 h day length, 22°C day and 18°C night temperatures, with 60% relative humidity and a light intensity of 460 mE. DNA extracted from this tissue was used for both long read Nanopore and short read Illumina sequencing. For Nanopore sequencing, nuclei were extracted from the floral bud tissue following Lu et al. (2017), with minor modifications. We ground 1–1.5 g of floral bud tissue into a coarse powder in liquid nitrogen. Ground tissue was resuspended in LB01 buffer (15 mM Tris pH 7.5, 2 mM EDTA (Ethylenediaminetetraacetic acid), 80 mM KCl, 20 mM NaCl, 15 mM 2-Mercaptoethanol, 0.15% Triton-X 100 and 0.5 mM Spermine) on ice with intermittent mixing. Tissue homogenate was then filtered through four layers of miracloth (EMD Millipore Corp.) followed by filtration through a 20 μm cell strainer (pluriStrainer). Filtrate was carefully pipetted on top of equal volume density gradient centrifugation buffer (1.7 M Sucrose, 10 mM Tris–HCl pH 8.0. 2 mM MgCl2, 5 mM 2-Mercaptoethanol, 1 mM EDTA, 0.15% Triton-X 100) in a 50 mL falcon tube and centrifuged at 2500 g for 30 min at 4°C. After centrifugation, the supernatant was decanted and the nuclei pellet was used to isolate high-molecular weight (HMW) DNA using the Nanobind Plant Nuclei Big DNA kit (Circulomics, Baltimore, MD, Cat # NB-900-801-01).

2.1.1 | Oxford Nanopore PromethION Sequencing

Population genetic methods based on short read sequencing have recently been used to identify large regions of suppressed recombination that have the potential to be chromosomal rearrangements (Todesco et al. 2020). Although these methods are efficient, they cannot confirm the existence of inversions, capture the full complement of DNA within inversions, or pinpoint inversion breakpoints. Doing so requires long-read sequencing. To achieve this, we performed Oxford Nanopore Technologies (ONT) sequencing. Nanopore libraries were prepared using the Oxford Nanopore SQK-LSK110 Ligation Sequencing Kit and loaded onto a FLO-PRO002 (vR9.4.1) flow cell. Sequencing was carried out on a PromethION sequencer (21.02.7) for 96 h, followed by basecalling with the Nanopore Guppy basecaller software (v4.3.4). We obtained 12,580,640 (120.74 GB) and 13,106,600 (133.36 GB) nanopore reads for LMC-L1 and SWB-S1, respectively, with median read lengths of 6.1 kb and 7.7 kb. Quality trimming resulted in 9,255,001 reads for LMC-L1 (337x coverage) and 9,423,361 reads for SWB-S1 (360x coverage), with 73.6% and 71.9% of reads passing filtering for LMC-L1 and SWB-S1, respectively.

2.1.2 | Illumina Sequencing

We polished the genome assembly and performed SNP calling using short-read sequencing. DNA was extracted from unopened floral buds using a DNeasy Plant Mini Kit (Qiagen) and prepped with the Illumina TruSeq Nano DNA Library preparation kit. Sequencing was conducted on one lane of an Illumina NovaSeq 6000 S4 flow (2×150) using a NovaSeq V1.5 300-cycle reagent kit. Base calling was done with Illumina RTA v3.4.4, and the output was demultiplexed and converted to FastQ format using Bcl2fastq v2.20.0.

2.1.3 | Oxford Nanopore PromethION Assembly, Polishing and Scaffolding

Adapters were removed from the reads using Porechop v0.2.5 (https://github.com/rrwick/Porechop) and quality filtered using NanoLyse and Nanofilt (–q 0 and –l 300). We removed possible contaminants using a microbe genebank (genbank-k31.sbt.json). *De novo* genome assembly was conducted with Flye v2.9.1 (Kolmogorov et al. 2020), followed by two rounds of polishing using Racon (v1.5.0) (Vaser et al. 2017) and a single round of Medaka (https://github.com/nanoporetech/medaka). The genome was finished with two rounds of Pilon (Walker et al. 2014) polishing using the Illumina sequencing. We checked for misassembly using Tigment-long (Jackman et al. 2018). Scaffolding into chromosomes was initially performed using Allmaps (Tang et al. 2015) by combining genetic map data (Lowry and Willis 2010) and synteny to the IM62, TOL and NONTOL genomes (phytozome-next.jgi.doe.gov). Additional contigs were added to the chromosomes through an iterative process using ragtag (Alonge et al. 2022) and lrscaf (Qin et al. 2019), combined with manual inspection and correction. Genome assembly statistics were calculated using assembly-stats (v1.0.1, https://github.com/sanger-pathogens/assembly-stats). Completeness of the genome assembly was verified throughout the pipeline using BUSCO v2.0 (Simão et al. 2015) and the LTR Assembly Index (LAI) pipeline (Ou et al. 2018).

2.1.4 | Gene Annotations

Genes were annotated using the MAKER pipeline (Cantarel et al. 2008; Holt and Yandell 2011). Support for gene models was provided by transcripts assembled from RNA-seq and protein alignments. Illumina reads were trimmed for adapter sequences using trimmomatic (v0.39; Bolger et al. 2014) and aligned to their respective genomes using HISAT2 (v2.2.1; Kim et al. 2019). PacBio reads were aligned by minimap2 (v2.24; Li 2018; Phytozome v13 n.d.). Transcripts were assembled by

StringTie2 (v2.2.1; Kovaka et al. 2019). For protein alignments, protein sequences from *Arabidopsis thaliana* (Araport11; Cheng et al. 2017), *Oryza sativa* (v7; Kawahara et al. 2013), *Solanum lycopersicum* (ITAG4.0; Hosmani et al. 2019), and UniProtKB/Swiss-Prot plants (release-2022_02; Schneider et al. 2005) were aligned to each genome using Exonerate protein2genome (Slater and Birney 2005). Repeatmasker (v4.1.1; RepeatMasker Home Page n.d.) was used to soft-mask the genome using TE sequences identified by Extensive *de-novo* TE Annotator (EDTA, see TE Annotations). An initial round of MAKER was run using the soft-masked genome and gff files from the transcriptome assembly and protein alignment. Annotations from this initial round of MAKER were then used to train SNAP (v2013_11_29; Korf 2004) and AUGUSTUS (v3.4.0; Stanke and Morgenstern 2005). To prevent overfitting, only 600 randomly sampled MAKER annotations were used to train AUGUSTUS. MAKER was then run a second time using models from SNAP and AUGUSTUS. To identify putative genes missed by MAKER in either genome, we next used Liftoff (v1.6.3; Shumate and Salzberg 2020) to transfer annotations from one genome onto the other. Lifted annotations were then filtered using GffCompare (v0.11.2; Pertea and Pertea 2020) to remove annotations with significant overlap to existing MAKER annotations. Remaining lifted annotations with valid open reading frames (ORF; 'valid_ORFs = 1' or 'valid_ORF = True' in the GFF attributes column) were considered as putative genes, while those without a valid ORF ('valid_ORFs = 0' or 'valid_ORF=False' in the GFF attributes column) were considered putative pseudogenes. This process was repeated using annotations from the reference IM62 (v2.0; Hellsten et al. 2013) genome annotation. Genes were flagged as potentially misannotated transposons as described previously (Bowman et al. 2017), with the exclusion of searching of Gypsy HMM profiles, as we found that this led to too many real genes being excluded. Given the often blurry line between genes and transposons, we retained these gene models in the annotation and simply flagged them as possible transposons.

2.1.5 | Gene Function

Gene functions were assigned by first searching for PFAM domains using InterProScan (v5.57–90.0) and then identifying the top five hits with DIAMOND BLASTX against Arabidopsis TAIR10 proteins (e-value cutoff 1e-6). Results were integrated using a custom script from Kevin Childs (available at https://github.com/niederhuth/mimulus-assembly).

2.2 | Structural Variant and SNP Calling and Annotation

Pseudo-chromosome assemblies were aligned to each other using MUM&Co (*v3.0.0*; O'Donnell and Fischer 2020), switching the reference and query, for calling SVs for each line. SVs were called via the whole genome alignment approach using MUM&Co. SVs (inversions, deletions, insertions and duplications) were quality filtered to ≥ 50 bp. Lastly, we removed called insertions and deletions with a continuous strand of 'NNN', as these segments represent gaps created by RagTag and are likely false positives. We purposely do not include translocations as many of the called translocations were likely artefact. SVs were annotated using BEDtools *intersect* (Quinlan and Hall 2010) to identify overlapping genes and structural variants. Many of the larger structural variants we focus on here were previously identified in the literature (Holeski et al. 2014; Lowry and Willis 2010) or suspect inversions (Flagel et al. 2019). In some cases, MUM&CO (O'Donnell and Fischer 2020) failed to detect these larger structural variants, and therefore, we used synteny plots to confirm their presence.

To call SNPs, we aligned the Illumina whole genome sequence data of each line to the reference genome of the other line. We quality trimmed using Trimmomatic v0.39 (Bolger et al. 2014) to a minimum length of 50 bp and a quality of phred33. We used BWA-MEM2 (Vasimuddin et al. 2019) to align SWB-S1 reads to the inland annual genome (98.63% alignment rate) and LMC-L1 reads to the coastal perennial (98.3% alignment rate) genome. SNPs were called using GATK (McKenna et al. 2010). We marked duplicates using PICARDTOOLS' *MarkDuplicates* function and then used GATK's *HaplotypeCaller* to call SNPs in individual samples. We then genotyped the SNPs using GATK's *GenotypeGVCF* and filtered them using *VariantFiltration*.

SNPs were annotated using ANNOVAR (Wang et al. 2010) and filtered to includeframeshift insertions, frameshift deletions, stop loss, stop gain and splicing. ANNOVAR (Wang et al. 2010) was used to identify synonymous and nonsynonymous SNPs. To estimate a rate of synonymous substitutions at 4-fold degenerate sites, we identified 4-fold degenerate sites using degenotate (https://github.com/harvardinformatics/degenotate.git). We intersected the synonymous SNPs with the list of 4-fold degenerate sites using bedtools *intersect* (Quinlan and Hall 2010).

We also reanalyzed the pooled sequencing data from Gould et al. (2017) following the same methods as in that study, but using our new genome assemblies as references (Data S1, supplementary methods 2). Briefly, this analysis involved the comparison of whole genome pooled sequencing data from 101 coastal perennial accessions with pooled sequencing data from 92 inland annual accessions (Gould et al. 2017). Following read processing and alignment (see Data S1, supplementary methods 2), we split the genome into 1000 called base pair windows. We removed windows where the average depth of coverage exceeded two standard deviations from the mean of all window depths. This reduced the number of SNPs called due to mapping errors in repetitive regions. The G statistic and π-ratio (inland annual π/coastal perennial π) were calculated for each window.

2.3 | Synteny, PAVs, CNVs and Inversion Breakpoints

Our new genome assemblies made it possible to localise the region of the inversion breakpoints for the inv_chr8A inversion. Due to the complex repetitive nature of the genome in the region of the inversion breakpoints, we could not identify the exact nucleotide sites of the breakpoint mutation. For the purpose of this study, we define each breakpoint region

as extending from the gene closest to the breakpoint outside of the inversion to the second closest gene to the breakpoint within the inversion (Data S1, Figure S13). To identify a stringent set of syntenic genes between ecotypes in the regions around the breakpoints, we implemented GENESPACE (Lovell et al. 2022), a pipeline that uses both OrthoFinder (Emms and Kelly 2015; Emms and Kelly 2019) and blastp. For all estimates of sequence level differences, we used the first base pair of the first gene of the inverted syntenic block to the last gene of the inverted syntenic block. In addition to inv_chr8A, we were able to localise the boundaries of another previously known inversion on chromosome 5 (inv_chr5A), as well as two previously unknown large inversions and many small inversions. These newly identified inversions include a smaller inversion nested within inv_chr8A (inv_chr8B) and a large inversion on chromosome 14 (inv_chr14A). For all of these inversions, the repetitive nature of the region around the inversion breakpoints made it challenging to define the exact nucleotide of the breakpoint mutation. While we could not identify exact breakpoints, we could define which genes were closest to both sides of each breakpoint. We used outputs from GENESPACE to identify copy number variations (CNVs) and presence-absence variants (PAVs) within the inversions and across the genomes using a custom script (https://github.com/niederhuth/mimulus-assembly).

To examine whether gene expression might have been disrupted by the inversion breakpoint mutations, we evaluated transcript abundances of genes in close proximity to the inversion breakpoints. Within the inversion, we focused this analysis on the two genes most proximal to the inversion breakpoints. Outside of the inversion, we only evaluated transcript abundance for the most proximal gene to each inversion breakpoint (Data S1, Figure S13). Transcript abundance data for this analysis was obtained from Gould et al. (2018) (Data S1, supplementary methods 3).

2.3.1 | qRT-PCR of *GA20ox2* (AT5G51810, Migut.H00683)

To determine whether expression differences in *GA20ox2* might contribute to phenotypic differences between ecotypes, we conducted qRT-PCR because this gene is expressed at a level too low to be analysed with RNA-seq. We extracted RNA from three biological replicates of leaf tissue and the floral shoot apex from wild-type LMC-L1 and SWB-S1 plants using the Spectrum Plant Total RNA Kit (Sigma). cDNA was synthesised for each sample using GoScript Reverse Transcription Mix, Oligo(dT) (Promega). We performed qRT-PCR using Power SYBR Green PCR master mix (Applied Biosystems) on a CFX96 touch real-time PCR machine (Bio-Rad). The PCR programme was as follows: 40 cycles at 95°C for 15 s and 60°C for 30 s. We determined amplification efficiencies for each primer pair using a dilution series (1:2, 1:4, 1:8, 1:16) of pooled cDNA samples. We used *UBC*, the ubiquitin-conjugating enzyme gene, as a reference gene to calculate the relative expression of *GA20ox2* using the formula $(E_{ref})^{CP(ref)}/(E_{target})^{CP(target)}$ (Pfaffl 2001). No differential expression was found for leaf tissue, and these results are not reported (two-tailed Student's *t*-test, $p > 0.05$).

3 | Results

3.1 | De Novo Assembly of *M. guttatus* Inland Annual and Coastal Perennial Lines

The final, polished genome assemblies were approximately 277 Mbps (335X coverage ONT and 150X coverage WGS) spanning 1198 contigs for LMC-L1 (inland annual) and 278 Mbps (365X coverage ONT and 151X) spanning 707 contigs for SWB-S1 (coastal perennial). Both assemblies demonstrated high contiguity with a contig N50 of 5.83 Mbps (LMC-L1) and 4.90 Mbps (SWB-S1) and a scaffold N50 of 18.2 Mbps (LMC-L1) and 18.8 Mbps (SWB-S1). Based on genetic maps and synteny, we assembled 93.0% of the LMC-L1 bps and 93.7% of the SWB-S1 sequence into 14 chromosomes (Hellsten et al. 2013). Our genomes recovered more than 98% of the eudicot set of BUSCO (Simão et al. 2015) orthologs (eudicots_odb10), an improvement from 96.9% in the previously available *M. guttatus* genome assembly (Hellsten et al. 2013) IM62 v2; (Hellsten et al. 2013). The LTR Assembly Index (LAI), an independent assessment of assembly quality based on the completeness of assembled LTR retrotransposons (Ou et al. 2018), was much higher in both LMC-L1 (13.47) and SWB-S1 (16.28) than the IM62 v2 reference (8.79), indicating a more complete assembly of repetitive regions (Data S1, Table S1).

We annotated a total of 27,583 genes in LMC-L1 and 26,876 genes in SWB, in comparison to 28,140 genes in IM62 v2 (Hellsten et al. 2013) (Data S1, Table S1). We compared the LMC-L1 and SWB-S1 genomes using *GENESPACE* (Lovell et al. 2022), identifying 19,245 syntenic genes between LMC-L1 and SWB-S1 (Data S1, Table S2). Additionally, in LMC-L1, we found 5105 presence-absence variants (PAVs), 3026 pseudogenes and 1411 tandem duplicates. In SWB-S1, we found 4707 PAVs, 3110 pseudogenes and 1401 tandem duplicates.

3.2 | Genome-Wide SNPs and Structural Variants

To identify larger structural variants (SVs) between the LMC-L1 and SWB-S1 genomes, we used MUM&CO, a whole genome alignment method (O'Donnell and Fischer 2020). The number of SVs between the LMC-L1 and SWB-S1 genomes is reported in Data S1, Table S3. Across the genome, there were 12,013 genes associated with structural variants in LMC-L1 (variants affecting genes: 1379 insertions, 8493 deletions, 72 duplications and 2069 inversions) and 11,582 genes associated with structural variants in the SWB-S1 (variants affecting genes: 1375 insertions, 8300 deletions, 51 duplications and 1856 inversions).

To identify SNPs between the LMC-L1 and SWB-S1 accessions, we aligned whole genome sequencing (WGS) from one accession to the other accession's reference genome. From these alignments, we focused on the evolution of coding regions by identifying high impact SNPs, which include the following variant types: stop codon gain (2787 in SWB-S1 and 2638 in LMC-L1), stop codon loss (723 in SWB-S1 and 700 in LMC-L1), frameshift deletion (7299 in SWB-S1 and 7541 in LMC-L1), frameshift insertion (7002 in SWB-S1 and 6951 in LMC-L1) and splicing (3986 in SWB-S1 and 3392 in LMC-L1). We also identified all other synonymous and

nonsynonymous SNPs. All coding region SNPs are reported for both genomes in Data S1, Tables S4 and S5.

3.3 | Identification of Large Chromosome Inversions and Their Breakpoints

The assembly of the nanopore long-read genomes allowed us for the first time to identify large chromosomal inversions from sequencing data alone as well as identify the locations of the breakpoint mutations that formed these inversions in the first place. The locally adaptive Inv_chr8A was found to span 6.7 Mb in LMC-L1 and 5.6 Mb in SWB-S1 (Figure 1A, Data S1, Figure S1 and Table S5). In addition, our analysis led to the discovery of a large inversion nested within inv_chr8A. This nested inversion (inv_chr8B) spans 213,792 bps in LMC-L1 and 261,302 bps in SWB-S1 (Figure 1B, Data S1, Figure S1 and Table S5). Beyond chromosome 8, we were able to localise a previously identified inversion on chromosome 5 (inv_chr5A), which is approximately 4.2 Mb long in LMC-L1 and 4.0 Mb in SWB-S1 (Figure 1A, Data S1, Figure S1 and Table S5). While we have successfully identified inv_chr5A from our genome assemblies, it is located near the end of the chromosome arm, and there are gaps within the inversion in LMC-L1 of the assemblies. Therefore, there is uncertainty about the location of this inversion's breakpoint toward the end of the chromosome. Finally, we identified a fourth large inversion on chromosome 14 (inv_chr14A), which was previously unknown. The inv_chr14A inversion has an approximate size of 2.4 Mb in LMC-L1 and 2.8 Mb in SWB-S1 (Figure 1A, Data S1, Figure S1 and Table S5).

Because of the differences in the size of the inversion regions in the two genome assemblies, we were curious whether there were any major differences in gene content between the inversion orientations. Our analyses revealed striking differences in gene content. Inv_chr8A (including inv_chr8B) had 177 LMC-L1-specific genes, 125 SWB-S1-specific genes and 613 genes shared between the two genomes. Inv_chr8B shares 36 genes between the genomes but has 9 LMC-L1-specific genes and 8 SWB-S1-specific genes. Inv_chr5A had a total of 113 LMC-L1-specific genes and 90 SWB-S1-specific genes but shared 396 genes between the LMC-L1 and SWB-S1. Lastly, the chromosome 14 inversion had 247 LMC-L1-specific genes, 308 SWB-S1-specific genes and 1133 shared genes. Many of these large gene content differences are due to PAVs and copy number variants (CNVs) which we discuss in the following paragraph. Errors in gene annotations could also contribute to PAVs and CNVs and thus our estimated gene content differences.

While previous studies have demonstrated the role of inv_chr8A in local adaptation (Lowry and Willis 2010) and implicated inv_chr5A (Gould et al. 2017), our improved assemblies now capture the full complement of genes within these inversions and make it possible to identify candidate genes that could have driven the geographic distributions of these inversions. In the following section, we highlight genetic differences between inversion orientations. CNVs, including PAVs, could explain both differences in inversion size and phenotypic differences. Within inv_chr8A, there were 338 CNVs, with 302 being PAVs; in inv_chr8B, there were 19 CNVs, with 17 being PAVs. Within inv_chr5A, there were 227 CNVs, with 203 being PAVs. Within inv_chr14A, there were 100 CNVs, with 84 being PAVs. Some of these CNVs in

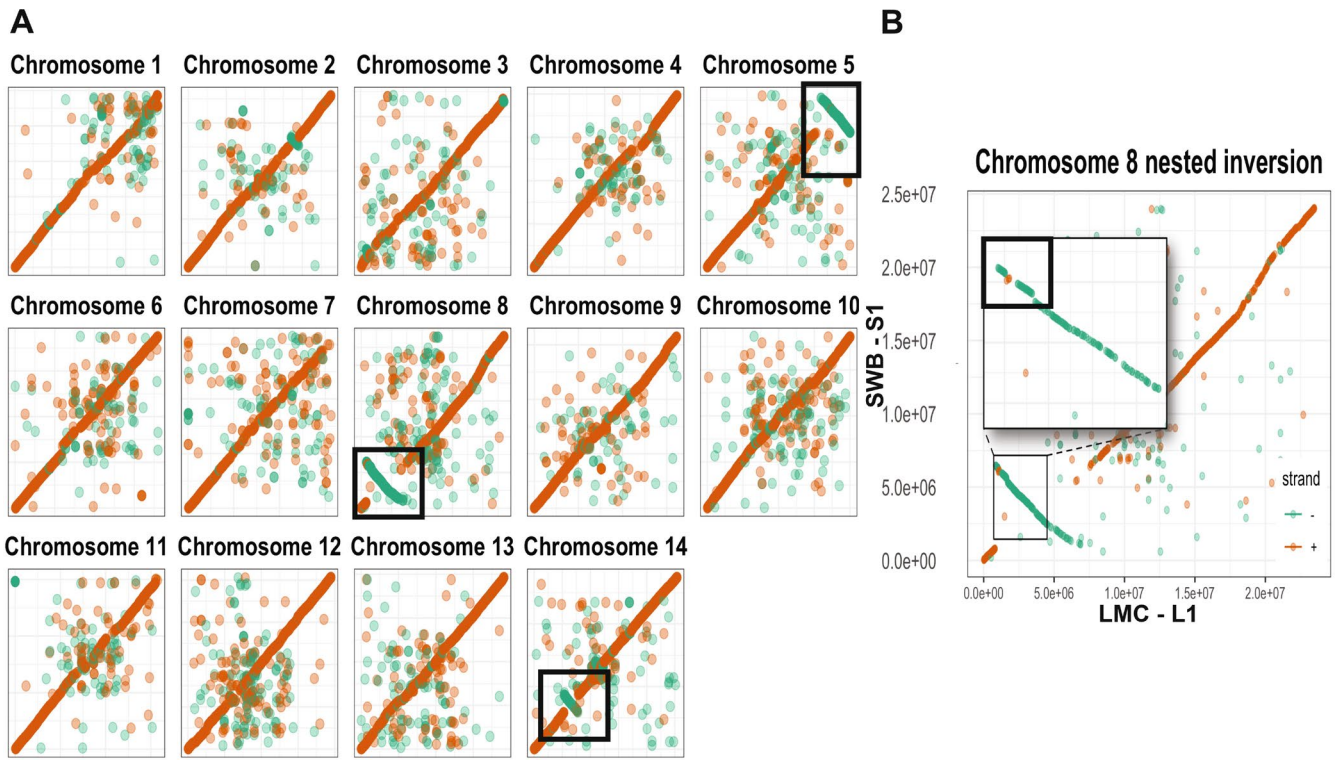

FIGURE 1 | (A) Whole genome alignment of all 14 chromosomes between the SWB-S1 and LMC-L1 genomes. Large inversions on chromosomes 5, 8 and 14 are visible in the dotplots (highlighted with boxes outlined in black), where the teal dots represent the negatively oriented strands while orange represent positively oriented strands. (B) The inv_chr8B captured within inv_chr8A.

the inversions could be explained by genes becoming pseudogenized within the inversion. In inv_chr8A, including inv_chr8B, there were 90 pseudogenes in LMC-L1 and 74 pseudogenes in SWB-S1 (Data S1, Table S6). Inv_chr8B included 6 pseudogenes in LMC-L1 and 8 pseudogenes in SWB-S1 (Data S1, Table S6). Within inv_chr5A, there were 54 pseudogenes in LMC-L1 and 43 pseudogenes in SWB-S1 (Data S1, Table S6). Lastly, within inv_chr14A, there were 22 pseudogenes in LMC-L1 and 19 pseudogenes in SWB-S1 (Data S1, Table S6). We report SNPs (all SNPs, high impact SNPs, and synonymous and nonsynonymous SNPs) falling within the chromosome inversions in Data S1, Tables S4 and S5. These SNPs were identified from WGS comparison of the SWB-S1 and LMC-L1 genomes.

3.4 | Evolutionary Histories of Large Inversions

To determine which inversion orientations are ancestral, we implemented GENESPACE (Lovell et al. 2022) using *Mimulus lewisii*, a distant relative, as the reference genome for comparison (http://mimubase.org/FTP/Genomes/) (Data S1, Figure S2). From this analysis, we reasoned that inversions sharing the same orientation as *M. lewisii* are in the ancestral orientation. We found the orientations of inv_ch5A (Data S1, Figure S3), inv_chr8A (Data S1, Figure S4) and inv_chr8B (Data S1, Figure S4) to be ancestral in LMC-L1. SWB-S1 has the ancestral orientation for inv_chr14A (Data S1, Figure S5). The results for inv_chr8A are consistent with the results found by Coughlan et al. (2021).

In addition to identifying which inversion orientation is ancestral, we were interested in the relative ages of inversion polymorphisms. Here, we compared the level of divergence between the LMC-L1 and SWB-S1 genomes for inverted regions and to the rest of the genome. When an inversion first forms, the two orientations of an inversion should have similar levels of divergence as the rest of the genome. As an inversion ages, each orientation should accumulate genetic changes that lead to elevated levels of divergence. To evaluate the relative ages of each inversion, we aligned Illumina reads from LMC-L1 to the SWB-S1 genome and aligned reads from SWB-S1 to the LMC-L1 genome. We then compared the levels of divergence at 4-fold degenerate synonymous sites for each inversion. The genome-wide average divergence at 4-fold degenerate sites was 0.043, regardless of which genome was used as the reference (Data S1, Table 1). Both the inv_chr5A (LMC-L1 Illumina resequencing: 0.055, SWB-S1 Illumina resequencing: 0.061) and inv_chr8A (LMC-L1 Illumina resequencing: 0.057, SWB-S1 Illumina resequencing: 0.058) inversions had elevated divergence relative to the genome-wide average, which suggests that these inversions have been segregating within this species for a long time. The inv_chr14A had similar levels of 4-fold degenerate site divergence (LMC-L1 Illumina resequencing: 0.041, SWB-S1 Illumina resequencing: 0.037) as the genome-wide average, suggesting that it is a relatively new inversion. Interestingly, the smaller nested inversion (inv_chr8B) had very high levels of divergence (LMC-L1 Illumina resequencing: 0.084 SWB-S1 Illumina resequencing: 0.083, Data S1, Table 1), which suggests that it is much older than any of the other inversions.

In addition to directly comparing divergence between the SWB-S1 and LMC-L1 genomes, we were able to evaluate whether there were differences in ecotype-wide polymorphism using a previous population genetic dataset (Gould et al. 2017). We reanalyzed this data using our new LMC-L1 and SWB-S1 genome assemblies (Data S1, Methods). Given the improvements in the genome assemblies over the previous reference IM62 v2 genome (Hellsten et al. 2013), we anticipated potentially new patterns in sequence diversity and differentiation. This new analysis also allowed us to evaluate how reference bias in alignments can affect population genetic summary statistic estimation. Regardless of the reference genome, the inland annual ecotype had higher nucleotide diversity ($\pi = 0.040$ regardless of reference genome). In contrast, the coastal ecotype pool differed slightly in diversity based on

TABLE 1 | LMC-L1 and SWB-S1 SNPs called from WGS were annotated and filtered to include synonymous SNPs at 4-fold degenerate sites for each inversion and genome-wide.

Genotype	Location	4-fold degenerate SNPs	4-fold degenerate sites	4-fold degenerate SNPs/ 4-fold degenerate sites
LMC-L1	Genome-wide	174,745	4,106,234	0.043
LMC-L1	inv_chr5A	4497	81,202	0.055
LMC-L1	inv_chr8A	8030	139,941	0.057
LMC-L1	inv_chr8B	636	7569	0.084
LMC-L1	inv_chr14A	1634	39,641	0.041
SWB-S1	Genome-wide	176,470	4,093,796	0.043
SWB-S1	inv_chr5A	4772	78,850	0.061
SWB-S1	inv_chr8A	7954	136,834	0.058
SWB-S1	inv_chr8B	630	7633	0.083
SWB-S1	inv_chr14A	1555	42,095	0.037

Note: SNPs for LMC-L1 were called by aligning LMC-L1 WGS data to the SWB-S1 genome, and SWB-S1 SNPs were called by aligning SWB-S1 WGS data to the LMC-L1 genome.

the reference genome ($\pi = 0.032$ aligned to SWB-S1, $\pi = 0.034$ aligned to LMC-L1). The lower diversity of the coastal ecotype is consistent with prior studies and the hypothesis that the coastal ecotype was founded through a population bottleneck (Gould et al. 2017; Lowry et al. 2008) (Data S1, Figure S6).

The population genetic data (Gould et al. 2017) allowed us to better evaluate the recent evolutionary history of the four large inversions. First, we compared the allelic differentiation (G statistic) for each inversion versus the rest of the genome. Consistent with our analysis of four-fold degenerate divergence between the SWB-S1 and LMC-L1 genomes, the nested inv_chr8B inversion had the highest level of allelic differentiation between the ecotypes (Figure 2, Data S1, Figure S7 and Table 2). The inv_chr8A and inv_chr5A inversions also had higher allelic divergence than the genome-wide average. In contrast, the inv_chr14A inversion had similar levels of allelic differentiation as the rest of the genome. To evaluate whether any of the inversions had undergone a recent selective sweep, we compared the within-ecotype diversity (π) for the inverted region to the rest of the genome. The idea here is that a significant reduction of within-ecotype diversity for any of the inversions would be consistent with a recent selective sweep. To simplify this analysis, we calculated the ratio of π (π inland annual pool/π coastal perennial pool) for windows across the genome. A π-ratio elevated above the genome-wide average (π-ratio = 1.25) would be consistent with a sweep within the coastal perennial ecotype, while a reduction in the π-ratio would be consistent with a sweep in the inland annual ecotype. Overall, the distribution of π-ratios was similar for inv_chr5A, inv_chr8A and inv_chr14A (Figure 2, Data S1, Figure S6 and Table 2). In contrast, the distribution of the π-ratio was significantly elevated for the nested inv_chr8B inversion, suggesting the possibility of a recent selective sweep in the coastal perennial ecotype.

3.5 | Candidate Genes for Inversion Supergene Effects

With localization of the inversion breakpoints for inv_chr8A and inv_chr8B, we were able to localise candidate genes that could underlie the phenotypic effects of inversions. We identified genes likely affected by divergent selection as those with outlier (top 1%) windows for the G statistic (explained above). Across the genome, the top windows for G contained 753 LMC-L1 and 635 SWB-S1 genes and/or their promoters and transcription start site (TSS) regions or 3′ untranslated regions (UTR). Many of these outlier genes, promoters, TSS regions and 3′ UTRs were syntenic between the LMC-L1 and SWB-S1 genomes, including 193 genes, 57 promoters and TSS regions and 90 3′ UTRs. Of these, 271 outlier windows were located within inv_chr8A (138 within inv_chr8B).

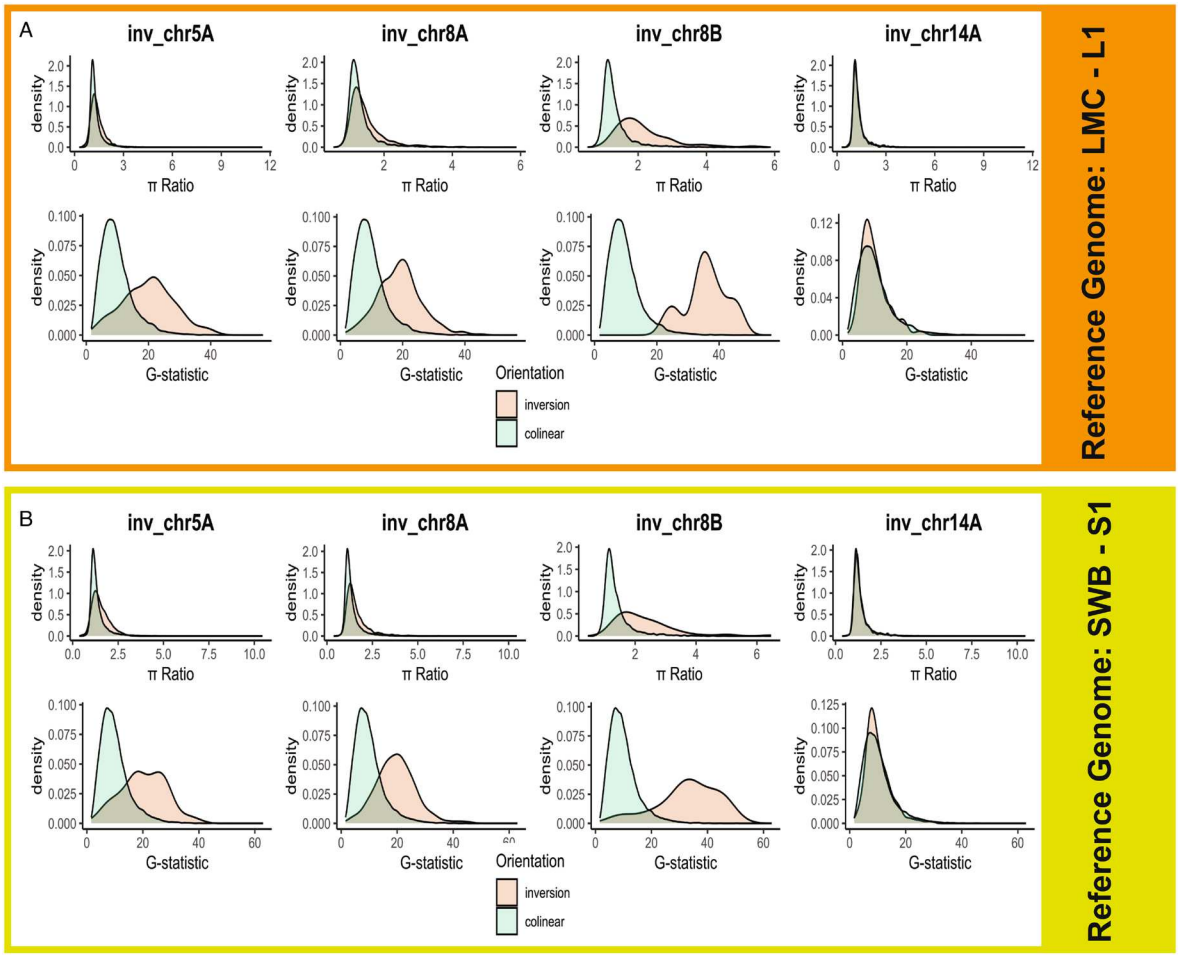

FIGURE 2 | G statistic and π ratio for each of the inversions (salmon) compared to the non-inverted (teal) sequence of the same chromosome when aligned to the LMC-L1 Genome (A) and to the SWB-S1 genome (B). Both the G statistic and π ratio were estimated across 1 kb windows.

TABLE 2 | Comparison of π and G statistic across the genome and for each inversion.

Reference genome	Location	π IA	π CP	π ratio	G statistic
SWB-S1	Colinear regions of chromosome 5	0.040	0.032	1.26	9.98
SWB-S1	inv_chr5A	0.040	0.029	1.41	20.28
SWB-S1	Colinear regions of chromosome 8	0.040	0.032	1.25	9.90
SWB-S1	inv_chr8A	0.041	0.028	1.48	20.07
SWB-S1	inv_chr8A (without inv_chr8B)	0.041	0.028	1.46	19.57
SWB-S1	inv_chr8B	0.042	0.021	2.02	32.88
SWB-S1	Colinear regions of chromosome 14	0.040	0.032	1.26	10.16
SWB-S1	inv_chr14A	0.041	0.033	1.25	10.09
SWB-S1	genome-wide	0.040	0.032	1.26	10.16
LMC-L1	Colinear regions of chromosome 5	0.043	0.037	1.18	8.19
LMC-L1	inv_chr5A	0.040	0.031	1.28	20.05
LMC-L1	Colinear regions of chromosome 8	0.040	0.033	1.21	10.70
LMC-L1	inv_chr8A	0.040	0.029	1.37	19.64
LMC-L1	inv_chr8A (without inv_chr8B)	0.040	0.030	1.35	18.71
LMC-L1	inv_chr8B	0.042	0.021	1.93	35.76
LMC-L1	Colinear regions of chromosome 14	0.039	0.031	1.23	11.03
LMC-L1	inv_chr14A	0.041	0.034	1.20	9.83
LMC-L1	genome-wide	0.040	0.034	1.20	10.01

Note: IA represents the inland annual pool and CP represents the coastal perennial pool.

One of the key outlier genes within inv_chr8A is *GA20ox2*, which codes for a structural gene in the gibberellin hormone synthesis pathway. *GA20ox2* (MgS1_08g02280) was an outlier for G and π ratio in our reanalysis using the SWB-S1 reference genome, which is similar to what Gould et al. (2017) found when using IM62 as the reference genome. We confirmed that *GA20ox2* is intact and expressed in both the SWB-S1 and LMC-L1 genomes by Sanger sequencing and qRT-PCR (Figure 3). In LMC-L1, expression of *GA20ox2* was ~1.7-fold higher in floral shoot apex compared to SWB-S1.

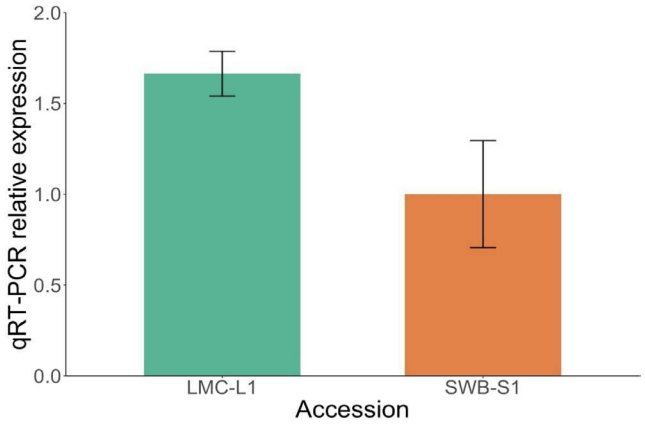

FIGURE 3 | Quantitative RT-PCR showing expression of *GA20ox2* in wild-type LMC-L1 and SWB-S1 floral shoot apex (three biological replicates). Error bars show standard deviation.

Another set of genes within inv_chr8A that could underlie the phenotypic differentiation of the ecotypes is a tandem array of *R2R3-MYB* genes within inv_chr8A (Cooley et al. 2011; Lowry et al. 2012). Previous work showed that calyx, corolla and leaf anthocyanin pigmentation traits differentiating the ecotypes also map to the region containing inv_chr8A (Lowry et al. 2012). It has been difficult to resolve the number of tandem copies of subgroup six *R2R3-MYBs* with previously available genome assemblies (i.e., IM62, TOL and NONTOL; phytozome-next.jgi.doe.gov/). Based on our CNV analysis, LMC-L1 and SWB-S1 have different numbers of copies of these *R2R3-MYB* genes. The LMC-L1 genome has five partial or complete copies of this gene, with three being flagged as pseudogenes (genes without valid open reading frames) in our analysis, while the SWB-S1 genome appears to have six partial or complete copies of this gene, none of which were called pseudogenes (Figure 4). Interestingly, the subgroup six *R2R3-MYB* genes appear syntenic with conserved directionality in LMC-L1 and SWB-S1, except for MgL1_08g06980, which is in the opposite orientation of all the other MYBs. This could indicate that it was duplicated independently. In investigating why some LMC-L1 copies were called pseudogenes, we found that MgL1_08g07004 matched perfectly to an annotation in IM62 (H00280), which is not annotated as an *R2R3-MYB* gene because it is missing distinguishing domains. However, MgL1_08g07004 almost perfectly matches MgL1_08g07000, especially in its intronic sequence, indicating that it is a partially duplicated gene.

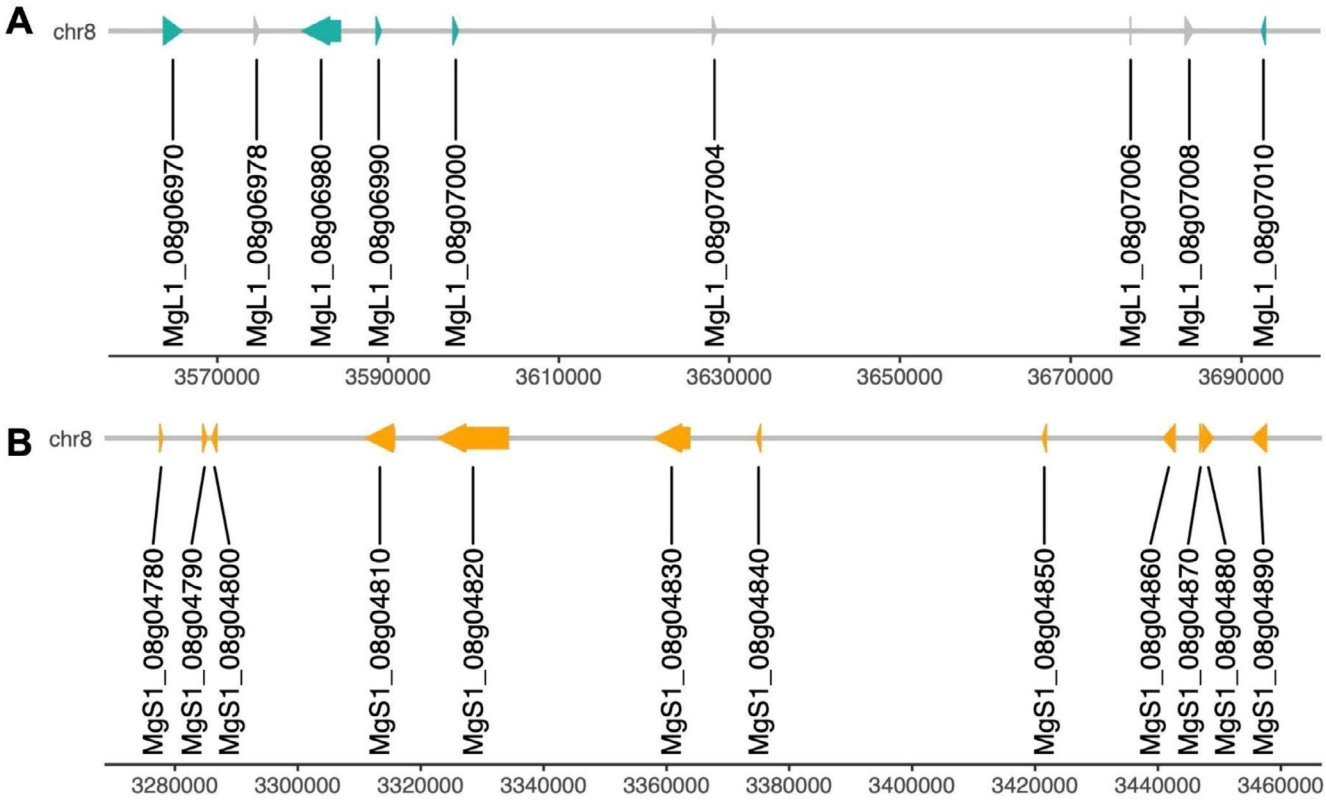

FIGURE 4 | The MYB region along chromosome 8 in LMC-L1 (A) and SWB-S1 (B). Each arrow (teal in LMC-L1 and orange in SWB-S1) represents a gene and orientation. The grey arrows represent pseudogenes.

3.6 | Genes Near Inversion Breakpoints Were Differentially Expressed

The identification of inversion breakpoints allows for the evaluation of whether breakpoint mutations could have disrupted genes in ways that could contribute to phenotypic effects. If an inversion breakpoint occurs within a gene, it would disrupt and likely eliminate that gene's function. Breakpoints occurring near genes can also cause changes in gene expression by disrupting or changing the position of *cis*-regulatory elements. Across all four inversions, we found no evidence that the breakpoint mutations had directly damaged the coding region of a gene. In terms of gene expression, we found that only seven out of 24 genes within the breakpoint regions (across four inversions) were differentially expressed. These differentially expressed genes include: MgL1_05g16120, L1_08g01750, MgL1_14g10910, MgS1_05g10260, MgS1_08g08930, MgS1_14g08050 and MgS1_14g08070 (Figure 5. Regardless, we did not find clear evidence to suggest the role of breakpoint mutations in causing phenotypic effects.

4 | Discussion

While chromosomal inversions are now well recognised as key factors in adaptive evolution, there is still much to be learned about how they evolve over time and what genetic mechanisms underlie their important phenotypic effects. In general, our results are consistent with the supergene hypothesis of inversion evolution and suggest that not only are multiple linked loci within the adaptive inversion contributing to its evolution, but that some of those loci may continue to evolve in response to local selective pressures in coastal versus inland habitats. The long-read sequencing assemblies that we report in this study also allowed us to localise three other large chromosomal inversions, each of which illustrates a key component of the evolution of inversions within species. This included the identification of the nested inversion (inv_chr8B) within inv_chr8A, which had not been identified in prior studies. Beyond chromosome 8, we were able to greatly improve the assembly of the inv_chr5A inversion, which was first reported in a cross between inland annual and coastal perennial lines (Holeski et al. 2014). The inv_chr5A inversion is suspected to play a role in adaptation based on elevated allelic differentiation of this region between coastal perennial and inland annual populations (Gould et al. 2018), which is a similar pattern to that for the locally adaptive inv_chr8A inversion. The inv_chr14A inversion was likely first detected by Flagel et al. (2019) as a 4 MB region of suppressed recombination. We were able to confirm that this region is, in fact, an inversion. Based on our analyses, inv_chr14A was less differentiated between the ecotypes, suggesting that it may be younger and/or not as geographically structured as the chromosome 5 and 8 inversions. Overall, the results of this study illustrate multiple important aspects of large inversion evolution, which we discuss below.

4.1 | The Evolution of Complex Nested Inversions

The biggest surprise of our study was the discovery of the relatively large inv_chr8B inversion (214–261 kb; depending on the genome) nested within the adaptive inv_chr8A inversion. The evolution of nested inversions is not unprecedented, but is also not

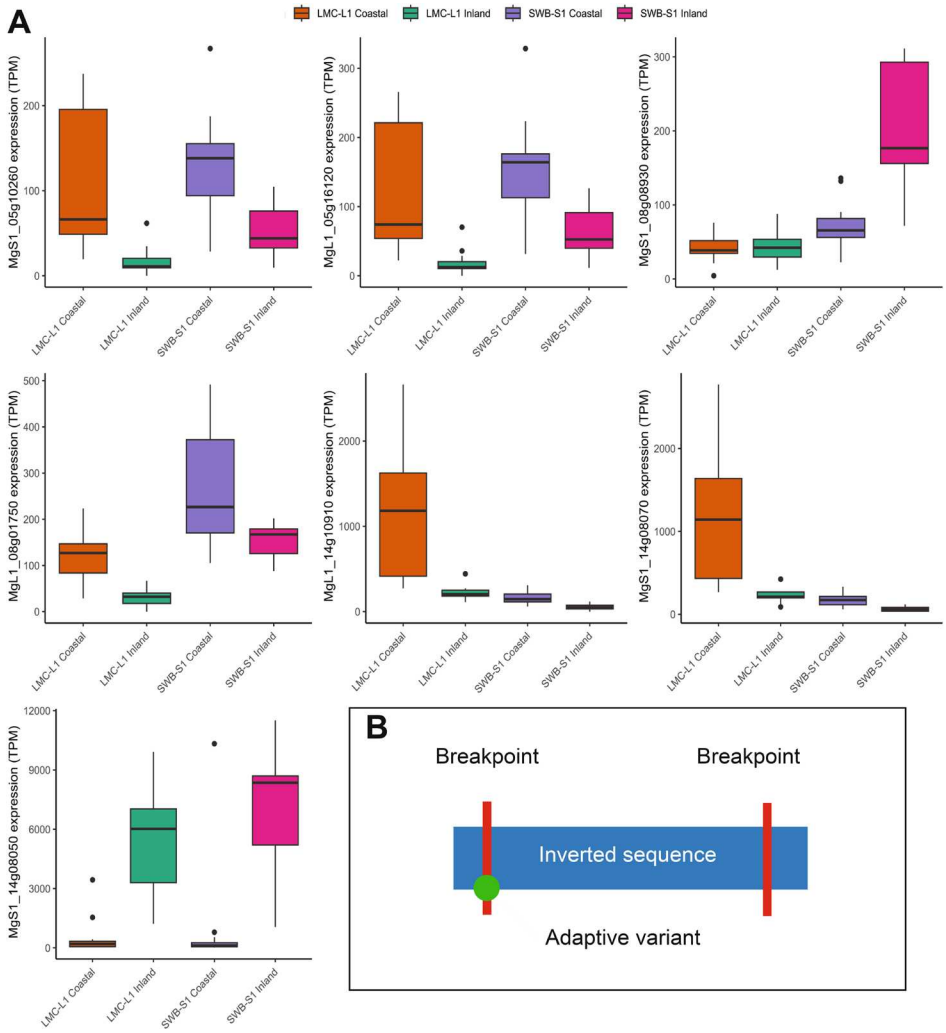

FIGURE 5 | (A) Differential expression represented in transcripts per million (TPM) in genes near the inversion breakpoints. Expression was quantified for plants grown at coastal and inland field sites, as described in Gould et al. (2018). Note, some plots are nearly identical because they are LMC-L1 and SWB-S1 orthologs (MgL14g10910 and MgS1_14g08070, MgS1_05g10260 and MgL1_05g16120). (B) A diagram depicting the inversion breakpoint hypothesis.

generally discussed in the context of locally adaptive inversions. Instead, nesting and clustering of multiple inversions in close proximity are typically associated with the evolution of sex chromosomes. For sex chromosomes, the accumulation of successive inversions and other rearrangements leads to contrasting levels of divergence (i.e., strata) for different regions of sex chromosomes, depending on the age of each region of suppressed recombination (Charlesworth 2023; Filatov 2022; Handley et al. 2004; Olito and Abbott 2023). This process eventually leads to distinct X/Y or Z/W chromosomes that no longer contain pseudoautosomal regions that recombine at all at meiosis when heterozygous (Bergero and Charlesworth 2009; Charlesworth 2023). Beyond sex chromosomes, studies in both maize and sunflowers have found evidence for large nested inversions (Dawe 2022; Mroczek et al. 2006; Todesco et al. 2020). In maize, nested inversions have been important for the evolution of chromosomal knobs that spread by meiotic drive (Dawe 2022; Mroczek et al. 2006). The significance of the autosomal nested inversions in sunflowers is unclear.

The entire region that includes both inversions on chromosome 8 is known to be involved in local adaptation to coastal perennial versus inland annual habitats (Lowry and Willis 2010). Given the geographic distribution of the larger inversion (inv_chr8A), it is also likely involved in adaptation to wetter versus drier habitats within inland regions (Lowry and Willis 2010; Oneal et al. 2014; Twyford and Friedman 2015). Therefore, natural selection is intimately involved in the spread of inv_chr8A. The question remains as to whether the smaller inv_chr8b inversion also confers habitat-dependent fitness advantages. The inv_chr8B inversion is particularly interesting, as it appears to be an ancient inversion that was later captured by the larger inv_chr8A inversion. These results suggest the intriguing possibility that inv_chr8B is itself an adaptive supergene that now contributes important phenotypic effects to the larger adaptive inv_chr8A supergene.

4.2 | The Role of Context-Dependent Suppressed Recombination in the Evolution of Adaptive Chromosomal Inversions

Inversions likely play a major role in adaptation because they suppress recombination in heterokaryotic individuals, while allowing for free recombination in homokaryotic individuals

(Berdan et al. 2023; Navarro et al. 1997). This dynamic means that locally adaptive alleles at distant loci on the same chromosome can be maintained in the same haplotypes for populations located in divergent habitats. At the same time, free recombination within each habitat allows for the purging of deleterious and maladapted alleles for the same genomic region within habitats (Berdan et al. 2021; Charlesworth 2012; Huang et al. 2022). Further, free recombination in each habitat minimises the interference of selection to act on multiple loci within that region through Hill–Robertson effects (Felsenstein 1974; Hill and Robertson 1966; Roze and Barton 2006). Our study, as well as a previous one (Gould et al. 2017), found evidence that *GA20ox2* has undergone a recent selective sweep within the coastal perennial ecotype, while much of the rest of the inv_chr8A region did not. This suggests that these loci can evolve independently of other parts of the inversion within ecotypes. Likewise, a recent study in sunflowers found that a high level of homozygosity for inversions minimised the mutational load in inverted regions (Huang et al. 2022). In both of these systems, adaptive inversion polymorphisms are thought to primarily occur in a homozygous state in alternative habitats, which facilitates recombination between loci within the inverted region. Overall, the ability of inversions to purge deleterious mutations and minimise Hill–Robertson effects gives inversions a major evolutionary advantage over other types of large regions of suppressed recombination, such as pericentromeric regions (Kuhl and Vader 2019; Wong and Filatov 2023).

4.3 | Candidate Genes Underlying the Adaptive Inversion's Phenotypic Effects

While holding together haplotypes of adaptive alleles across multiple genes through suppressed recombination is thought to be the primary reason for the association of inversions with local adaptation, evidence for this model is still lacking because multiple causative genes have not been identified for any inversion (Berdan et al. 2023). In *M. guttatus*, genes within inv_chr8A involved in the gibberellin (GA) hormone pathway are of particular interest because of the discovery that the addition of gibberellin (GA3) to coastal perennial plants leads them to develop more like inland annual plants by converting vegetative stolons into upcurved flowering branches (Lowry et al. 2019). Introgressing the inland annual orientation of the inversion into the coastal perennial background resulted in nearly identical phenotypic effects on branching and internode elongation as spraying coastal plants with GA3 (Lowry and Willis 2010). The GA gene, *GA20ox2*, is a top candidate gene for contributing to inv_chr8A's phenotypic effects. Not only were these genes allele frequency outliers in comparisons of perennial and annual populations, but *GA20ox2* was expressed at a higher level in the shoot apex of LMC-L1 than SWB-S1. *GA20ox2* expression is tissue- and time-specific, and we were not able to find evidence that it was expressed when analysing RNA-seq data from leaf tissue (Gould et al. 2017). In other systems (Andrés et al. 2014), *GA20ox2* is typically expressed in the floral shoot apex, similar to our findings in *M. guttatus*. Gould et al. (2018) collected tissue only from leaves, which could not detect the differential expression of *GA20ox2* in the floral shoot apex. In contrast, we found higher expression of *GA20ox2* in the floral apex for the inland annual than the coastal perennial line when we isolated RNA only from the floral shoot apex tissue. This expression pattern is consistent with the hypothesis that inland annuals flower earlier and have an upright growth architecture due to higher production of gibberellin hormones (Lowry et al. 2019).

While our study, as well as ongoing work, implicates a role for *GA20ox2* in the phenotypic effects of inv_chr8A, the supergene hypothesis requires that we identify multiple genes within the inversion that contribute to adaptive phenotypic divergence. A promising candidate for also contributing to adaptive phenotypic effects is the cluster of R2R3-MYB genes within inv_chr8A. A previous study mapped variation in five vegetative anthocyanin traits to the region inv_chr8A (Lowry et al. 2012), and coastal perennial and inland annual populations differ in anthocyanin pigmentation. While this gene cluster is promising, it has been difficult to link vegetative anthocyanin polymorphisms to evolutionary adaptations (Hatier and Gould 2008; Hughes et al. 2013; Hughes and Lev-Yadun 2023; Lee et al. 1979; Manetas 2006; Schaefer and Rolshausen 2006). In addition to this R2R3-MYB gene cluster, genes within the inv_chr8B inversion may play a role in the phenotypic effects of the locally adaptive inv_chr8A inversion.

4.4 | Little Evidence for a Role of Breakpoint Mutation in Causing the Phenotypic Effects of Adaptive Inversions

While the supergene hypothesis has been championed by evolutionary biologists in recent years, it is not the only mechanism by which inversions can contribute to adaptive phenotypic variation. Inversion mutations can also break genes or alter gene expression through mutations in promoters/enhancers or by changing the local chromatin architecture near breakpoints (Berloco et al. 2014; Elgin and Reuter 2013; Muller 1930; Nosil et al. 2020; Puig et al. 2015; Villoutreix et al. 2021; Vogel et al. 2009).

In this study, we found no evidence that the breakpoint mutations for the large inversions disrupted the coding regions of any genes. Instead, breakpoints were located primarily in gene-poor, repeat-rich regions of the genome. While we found no evidence that inversion breakpoint mutations broke any genes, it is possible that inversion mutations could have resulted in changing gene expression of nearby genes by disrupting promoter/enhancer elements or changing local chromatin landscapes. Indeed, we did find that seven of the genes located in close vicinity of the inversion breakpoints on chromosome 5 and 8 had significantly different levels of transcript abundance between SWB-S1 and LMC-L1 plants. From our study, we cannot establish whether the breakpoint mutation itself caused these differences in gene expression or if that regulatory divergence evolved later. Another recent study in *M. guttatus* also found little evidence for the breakpoint hypothesis of inversion evolution (Veltsos et al. 2024). Further, a recent study in *Drosophila* that created synthetic inversions at the position of naturally occurring inversion polymorphism did not cause any major effects on gene expression (Said et al. 2018). Likewise, (Kapun et al. 2023) found no greater elevation in gene expression for genes near the breakpoints of the *Drosophila* In(3R)Payne inversion versus elsewhere in the

inversion. These results collectively suggest that the evolution of gene expression divergence for inversions often happens over time, after the inversion breakpoint mutation, through the gradual accumulation of new mutations.

Author Contributions

L.M.K., D.B.L. and C.E.N. designed research; L.M.K., C.E.N., L.E.S. and S.K.K.R performed research, and L.M.K. and C.E.N. analysed data; and L.M.K., C.E.N., L.E.S. and D.B.L. wrote the paper.

Acknowledgements

This study was funded by the National Science Foundation (NSF) Plant Genome Research Program 2010769 to L.M.K. and 2109560 to L.E.S., Michigan State University Plant Biology start-up funds to C.E.N., and by two National Science Foundation Division of Integrative Organismal Systems Grants to D.B.L. (IOS-1855927 and IOS-2153100). We would like to thank Oxford Nanopore Technologies and the MSU Genomics Core for providing reagents and services that generated sequencing data that made this work possible. We would also like to thank Kevin Childs for guidance on genome annotation, Eleanore Ritter for guidance in detecting structural variants, and Lane Vitek for lab work.

Conflicts of Interest

The authors declare no conflicts of interest.

Data Availability Statement

Code for genome assembly can be found at https://github.com/niederhuth/mimulus-assembly and code for calling structural variants and SNPs, reanalysis of pooled sequencing and RNAseq, and figures can be found at https://github.com/Kollarlm/Breakpoint-mutations-supergene-effects-and-ancient-nested-rearrangements-in-yellow-monkeyflower.git. Raw ONT sequencing files are available through the NCBI Sequence Read Archive under project identifier PRJNA1047892—accessions SAMN38597945 (LMC-L1) and SAMN38597946 (SWB-S1). Raw RNA sequencing files are also available through the NCBI Sequence Read Archive under project identifier PRJNA1054563. The genome assemblies, annotations, TE annotations, and other supporting documents can be found on Dryad under DOI:10.5061/dryad.2ngf1vhwj.

References

Adrion, J. R., M. W. Hahn, and B. S. Cooper. 2015. "Revisiting Classic Clines in *Drosophila melanogaster* in the Age of Genomics." *Trends in Genetics* 31, no. 8: 434–444.

Alonge, M., L. Lebeigle, M. Kirsche, et al. 2022. "Automated Assembly Scaffolding Using RagTag Elevates a New Tomato System for High-Throughput Genome Editing." *Genome Biology* 23, no. 1: 258.

Anderson, A. R., A. A. Hoffmann, S. W. McKechnie, P. A. Umina, and A. R. Weeks. 2005. "The Latitudinal Cline in the In(3R)Payne Inversion Polymorphism has Shifted in the Last 20 Years in Australian *Drosophila melanogaster* Populations." *Molecular Ecology* 14, no. 3: 851–858.

Andrés, F., A. Porri, S. Torti, et al. 2014. "Short Vegetative Phase Reduces Gibberellin Biosynthesis at the Arabidopsis Shoot Apex to Regulate the Floral Transition." *Proceedings of the National Academy of Sciences of the United States of America* 111, no. 26: E2760–E2769.

Ayala, D., A. Ullastres, and J. González. 2014. "Adaptation Through Chromosomal Inversions in Anopheles." *Frontiers in Genetics* 5: 129.

Ayala, F. J., and M. Coluzzi. 2005. "Chromosome Speciation: Humans, *Drosophila*, and Mosquitoes." *Proceedings of the National Academy of Sciences of the United States of America* 102, no. Suppl 1: 6535–6542.

Beardmore, J. A., T. H. Dobzhansky, and O. A. Pavlovsky. 1960. "An Attempt to Compare the Fitness of Polymorphic and Monomorphic Experimental Populations of *Drosophila pseudoobscura*." *Heredity* 14, no. 1: 19–33.

Berdan, E. L., N. H. Barton, R. Butlin, et al. 2023. "How Chromosomal Inversions Reorient the Evolutionary Process." *Journal of Evolutionary Biology* 36: 1761–1782. https://doi.org/10.1111/jeb.14242.

Berdan, E. L., A. Blanckaert, R. K. Butlin, and C. Bank. 2021. "Deleterious Mutation Accumulation and the Long-Term Fate of Chromosomal Inversions." *PLoS Genetics* 17, no. 3: e1009411.

Bergero, R., and D. Charlesworth. 2009. "The Evolution of Restricted Recombination in Sex Chromosomes." *Trends in Ecology & Evolution* 24, no. 2: 94–102.

Berloco, M., G. Palumbo, L. Piacentini, S. Pimpinelli, and L. Fanti. 2014. "Position Effect Variegation and Viability Are Both Sensitive to Dosage of Constitutive Heterochromatin in *Drosophila*." *Genes, Genomes, Genetics* 4, no. 9: 1709–1716.

Bolger, A. M., M. Lohse, and B. Usadel. 2014. "Trimmomatic: A Flexible Trimmer for Illumina Sequence Data." *Bioinformatics* 30, no. 15: 2114–2120.

Bowman, M. J., J. A. Pulman, T. L. Liu, and K. L. Childs. 2017. "A Modified GC-Specific MAKER Gene Annotation Method Reveals Improved and Novel Gene Predictions of High and Low GC Content in *Oryza sativa*." *BMC Bioinformatics* 18, no. 1: 522.

Butlin, R. K., and T. H. Day. 1984. "The Effect of Larval Competition on Development Time and Adult Size in the Seaweed Fly, *Coelopa frigida*." *Oecologia* 63, no. 1: 122–127.

Cantarel, B. L., I. Korf, S. M. C. Robb, et al. 2008. "MAKER: An Easy-To-Use Annotation Pipeline Designed for Emerging Model Organism Genomes." *Genome Research* 18, no. 1: 188–196.

Charlesworth, B. 2012. "The Effects of Deleterious Mutations on Evolution at Linked Sites." *Genetics* 190, no. 1: 5–22.

Charlesworth, D. 2023. "Why and How Do Y Chromosome Stop Recombining?" *Journal of Evolutionary Biology* 36, no. 3: 632–636. https://doi.org/10.1111/jeb.14137.

Cheng, C.-Y., V. Krishnakumar, A. P. Chan, F. Thibaud-Nissen, S. Schobel, and C. D. Town. 2017. "Araport11: A Complete Reannotation of the *Arabidopsis thaliana* Reference Genome." *Plant Journal* 89, no. 4: 789–804.

Chouteau, M., V. Llaurens, F. Piron-Prunier, and M. Joron. 2017. "Polymorphism at a Mimicry Supergene Maintained by Opposing Frequency-Dependent Selection Pressures." *Proceedings of the National Academy of Sciences of the United States of America* 114, no. 31: 8325–8329.

Cooley, A. M., J. L. Modliszewski, M. L. Rommel, and J. H. Willis. 2011. "Gene Duplication in Mimulus Underlies Parallel Floral Evolution via Independent Trans-Regulatory Changes." *Current Biology* 21, no. 8: 700–704.

Coughlan, J. M., M. W. Brown, and J. H. Willis. 2021. "The Genetic Architecture and Evolution of Life-History Divergence Among Perennials in the *Mimulus guttatus* Species Complex." *Proceedings of the Royal Society B: Biological Sciences* 288: 20210077.

Coughlan, J. M., and J. H. Willis. 2019. "Dissecting the Role of a Large Chromosomal Inversion in Life History Divergence Throughout the *Mimulus guttatus* Species Complex." *Molecular Ecology* 28, no. 6: 1343–1357.

Darlington, C. D., and K. Mather. 1950. "The Elements of Genetics." *Population* 5, no. 2: 386.

Dawe, R. K. 2022. "The Maize Abnormal Chromosome 10 Meiotic Drive Haplotype: A Review." *Chromosome Research* 30, no. 2–3: 205–216.

Dobzhansky, T. 1936. "Position Effects on Genes." *Biological Reviews of the Cambridge Philosophical Society* 11, no. 3: 364–384.

Dobzhansky, T. 1947. "Adaptive Changes Induced by Natural Selection in Wild Populations of *Drosophila*." *Evolution* 1, no. 1/2: 1–16.

Dobzhansky, T. 1951. *Genetics and the Origin of Species*. 3rd ed. Columbia University Press.

Dobzhansky, T. 1970. *Genetics of the Evolutionary Process*. Columbia University Press.

Elgin, S. C., and G. Reuter. 2013. "Position-Effect Variegation, Heterochromatin Formation, and Gene Silencing in *Drosophila*." *Cold Spring Harbor Perspectives in Biology* 5: a017780.

Emms, D. M., and S. Kelly. 2015. "OrthoFinder: Solving Fundamental Biases in Whole Genome Comparisons Dramatically Improves Orthogroup Inference Accuracy." *Genome Biology* 16, no. 1: 157.

Emms, D. M., and S. Kelly. 2019. "OrthoFinder: Phylogenetic Orthology Inference for Comparative Genomics." *Genome Biology* 20, no. 1: 238.

Fang, Z., T. Pyhäjärvi, A. L. Weber, et al. 2012. "Megabase-Scale Inversion Polymorphism in the Wild Ancestor of Maize." *Genetics* 191, no. 3: 883–894.

Felsenstein, J. 1974. "The Evolutionary Advantage of Recombination." *Genetics* 78, no. 2: 737–756.

Filatov, D. A. 2022. "Recent Expansion of the Non-Recombining Sex-Linked Region on *Silene latifolia* Sex Chromosomes." *Journal of Evolutionary Biology* 35, no. 12: 1696–1708.

Flagel, L. E., B. K. Blackman, L. Fishman, P. J. Monnahan, A. Sweigart, and J. K. Kelly. 2019. "GOOGA: A Platform to Synthesize Mapping Experiments and Identify Genomic Structural Diversity." *PLoS Computational Biology* 15, no. 4: e1006949.

Friedman, J. 2014. "Genetic Determinants and Epistasis for Life History Trait Differences in the Common Monkeyflower, *Mimulus guttatus*." *Journal of Heredity* 105, no. 6: 816–827.

Gould, B. A., Y. Chen, and D. B. Lowry. 2017. "Pooled Ecotype Sequencing Reveals Candidate Genetic Mechanisms for Adaptive Differentiation and Reproductive Isolation." *Molecular Ecology* 26: 163–177. https://doi.org/10.1111/mec.13881.

Gould, B. A., Y. Chen, and D. B. Lowry. 2018. "Gene Regulatory Divergence Between Locally Adapted Ecotypes in Their Native Habitats." *Molecular Ecology* 27, no. 21: 4174–4188.

Hager, E. R., O. S. Harringmeyer, T. B. Wooldridge, et al. 2022. "A Chromosomal Inversion Contributes to Divergence in Multiple Traits Between Deer Mouse Ecotypes." *Science* 377, no. 6604: 399–405.

Hall, M. C., D. B. Lowry, and J. H. Willis. 2010. "Is Local Adaptation in *Mimulus guttatus* Caused by Trade-Offs at Individual Loci?" *Molecular Ecology* 19, no. 13: 2739–2753.

Handley, L.-J. L., H. Ceplitis, and H. Ellegren. 2004. "Evolutionary Strata on the Chicken Z Chromosome: Implications for Sex Chromosome Evolution." *Genetics* 167, no. 1: 367–376.

Harringmeyer, O. S., and H. E. Hoekstra. 2022. "Chromosomal Inversion Polymorphisms Shape the Genomic Landscape of Deer Mice." *Nature Ecology & Evolution* 6, no. 12: 1965–1979.

Hatier, J.-H. B., and K. S. Gould. 2008. "Foliar Anthocyanins as Modulators of Stress Signals." *Journal of Theoretical Biology* 253, no. 3: 625–627.

Hellsten, U., K. M. Wright, J. Jenkins, et al. 2013. "Fine-Scale Variation in Meiotic Recombination in Mimulus Inferred From Population Shotgun Sequencing." *Proceedings of the National Academy of Sciences of the United States of America* 110, no. 48: 19478–19482.

Hill, W. G., and A. Robertson. 1966. "The Effect of Linkage on Limits to Artificial Selection." *Genetical Research* 8, no. 3: 269–294.

Hoffmann, A. A., and L. H. Rieseberg. 2008. "Revisiting the Impact of Inversions in Evolution: From Population Genetic Markers to Drivers of Adaptive Shifts and Speciation?" *Annual Review of Ecology, Evolution, and Systematics* 39: 21–42.

Holeski, L. M., P. Monnahan, B. Koseva, N. McCool, R. L. Lindroth, and J. K. Kelly. 2014. "A High-Resolution Genetic Map of Yellow Monkeyflower Identifies Chemical Defense QTLs and Recombination Rate Variation." *Genes, Genomes, Genetics* 4, no. 5: 813–821.

Holt, C., and M. Yandell. 2011. "MAKER2: An Annotation Pipeline and Genome-Database Management Tool for Second-Generation Genome Projects." *BMC Bioinformatics* 12: 491.

Hosmani, P. S., M. Flores-Gonzalez, H. van de Geest, et al. 2019. "An Improved de Novo Assembly and Annotation of the Tomato Reference Genome Using Single-Molecule Sequencing, Hi-C Proximity Ligation and Optical Maps." *bioRxiv*: 767764. https://doi.org/10.1101/767764.

Huang, K., K. L. Ostevik, C. Elphinstone, et al. 2022. "Mutation Load in Sunflower Inversions Is Negatively Correlated With Inversion Heterozygosity." *Molecular Biology and Evolution* 39, no. 5: 101. https://doi.org/10.1093/molbev/msac101.

Huang, K., and L. H. Rieseberg. 2020. "Frequency, Origins, and Evolutionary Role of Chromosomal Inversions in Plants." *Frontiers in Plant Science* 11: 296. https://doi.org/10.3389/fpls.2020.00296.

Hughes, N. M., K. L. Carpenter, and J. G. Cannon. 2013. "Estimating Contribution of Anthocyanin Pigments to Osmotic Adjustment During Winter Leaf Reddening." *Journal of Plant Physiology* 170, no. 2: 230–233.

Hughes, N. M., and S. Lev-Yadun. 2023. "Review: Why Do Some Plants Have Leaves With Red or Purple Undersides?" *Environmental and Experimental Botany* 205: 105126.

Jackman, S. D., L. Coombe, J. Chu, et al. 2018. "Tigmint: Correcting Assembly Errors Using Linked Reads From Large Molecules." *BMC Bioinformatics* 19, no. 1: 393.

Jeong, H., N. M. Baran, D. Sun, et al. 2022. "Dynamic Molecular Evolution of a Supergene With Suppressed Recombination in White-Throated Sparrows." *eLife* 11: 79387. https://doi.org/10.7554/eLife.79387.

Joron, M., L. Frezal, R. T. Jones, et al. 2011. "Chromosomal Rearrangements Maintain a Polymorphic Supergene Controlling Butterfly Mimicry." *Nature* 477, no. 7363: 203–206.

Kapun, M., and T. Flatt. 2019. "The Adaptive Significance of Chromosomal Inversion Polymorphisms in *Drosophila melanogaster*." *Molecular Ecology* 28, no. 6: 1263–1282.

Kapun, M., E. D. Mitchell, T. J. Kawecki, P. Schmidt, and T. Flatt. 2023. "An Ancestral Balanced Inversion Polymorphism Confers Global Adaptation." *Molecular Biology and Evolution* 40, no. 6: 118. https://doi.org/10.1093/molbev/msad118.

Kawahara, Y., M. de la Bastide, J. P. Hamilton, et al. 2013. "Improvement of the *Oryza sativa* Nipponbare Reference Genome Using Next Generation Sequence and Optical Map Data." *Rice* 6, no. 1: 4.

Kim, D., J. M. Paggi, C. Park, C. Bennett, and S. L. Salzberg. 2019. "Graph-Based Genome Alignment and Genotyping With HISAT2 and HISAT-Genotype." *Nature Biotechnology* 37, no. 8: 907–915.

Kirkpatrick, M., and B. Barrett. 2016. "Chromosome Inversions, Adaptive Cassettes and the Evolution of Species' Ranges." In *Invasion Genetics*, 175–186. John Wiley & Sons, Ltd.

Kirkpatrick, M., and N. Barton. 2006. "Chromosome Inversions, Local Adaptation and Speciation." *Genetics* 173, no. 1: 419–434.

Kirkpatrick, M., and A. Kern. 2012. "Where's the Money? Inversions, Genes, and the Hunt for Genomic Targets of Selection." *Genetics* 190, no. 4: 1153–1155.

Kolmogorov, M., D. M. Bickhart, B. Behsaz, et al. 2020. "metaFlye: Scalable Long-Read Metagenome Assembly Using Repeat Graphs." *Nature Methods* 17, no. 11: 1103–1110.

Korf, I. 2004. "Gene finding in novel genomes." *BMC Bioinformatics* 5: 59.

Kovaka, S., A. V. Zimin, G. M. Pertea, R. Razaghi, S. L. Salzberg, and M. Pertea. 2019. "Transcriptome Assembly From Long-Read RNA-Seq Alignments With StringTie2." *Genome Biology* 20, no. 1: 278.

Kuhl, L.-M., and G. Vader. 2019. "Kinetochores, Cohesin, and DNA Breaks: Controlling Meiotic Recombination Within Pericentromeres." *Yeast* 36, no. 3: 121–127.

Kunte, K., W. Zhang, A. Tenger-Trolander, et al. 2014. "Doublesex Is a Mimicry Supergene." *Nature* 507, no. 7491: 229–232.

Lamichhaney, S., G. Fan, F. Widemo, et al. 2016. "Structural Genomic Changes Underlie Alternative Reproductive Strategies in the Ruff (*Philomachus pugnax*)." *Nature Genetics* 48, no. 1: 84–88.

Lee, D. W., J. B. Lowry, and B. C. Stone. 1979. "Abaxial Anthocyanin Layer in Leaves of Tropical Rain Forest Plants: Enhancer of Light Capture in Deep Shade." *Biotropica* 11, no. 1: 70–77.

Li, H. 2018. "Minimap2: Pairwise Alignment for Nucleotide Sequences." *Bioinformatics* 34, no. 18: 3094–3100.

Lovell, J. T., A. Sreedasyam, M. E. Schranz, et al. 2022. "Genespace Tracks Regions of Interest and Gene Copy Number Variation Across Multiple Genomes." *eLife* 11: 78526. https://doi.org/10.7554/eLife.78526.

Lowry, D. B., R. Cotton Rockwood, and J. H. Willis. 2008. "Ecological Reproductive Isolation of Coast and Inland Races of *Mimulus guttatus*." *Evolution* 62, no. 9: 2196–2214. https://doi.org/10.1111/j.1558-5646.2008.00457.x.

Lowry, D. B., D. Popovic, D. J. Brennan, and L. M. Holeski. 2019. "Mechanisms of a Locally Adaptive Shift in Allocation Among Growth, Reproduction, and Herbivore Resistance in *Mimulus guttatus*." *Evolution* 73, no. 6: 1168–1181.

Lowry, D. B., C. C. Sheng, J. R. Lasky, and J. H. Willis. 2012. "Five Anthocyanin Polymorphisms Are Associated With an R2R3-MYB Cluster in *Mimulus Guttatus* (Phrymaceae)." *American Journal of Botany* 99, no. 1: 82–91.

Lowry, D. B., and J. H. Willis. 2010. "A Widespread Chromosomal Inversion Polymorphism Contributes to a Major Life-History Transition, Local Adaptation, and Reproductive Isolation." *PLoS Biology* 8, no. 9: e1000500. https://doi.org/10.1371/journal.pbio.1000500.

Lu, Z., B. T. Hofmeister, C. Vollmers, R. M. DuBois, and R. J. Schmitz. 2017. "Combining ATAC-Seq With Nuclei Sorting for Discovery of Cis-Regulatory Regions in Plant Genomes." *Nucleic Acids Research* 45, no. 6: e41.

Lundberg, M., A. Mackintosh, A. Petri, and S. Bensch. 2023. "Inversions Maintain Differences Between Migratory Phenotypes of a Songbird." *Nature Communications* 14, no. 1: 452.

Lupski, J. R. 1998. "Genomic Disorders: Structural Features of the Genome Can Lead to DNA Rearrangements and Human Disease Traits." *Trends in Genetics* 14, no. 10: 417–422.

Manetas, Y. 2006. "Why Some Leaves Are Anthocyanic and Why Most Anthocyanic Leaves Are Red?" *Flora—Morphology, Distribution, Functional Ecology of Plants* 201, no. 3: 163–177.

Marquès-Bonet, T., M. Cáceres, J. Bertranpetit, T. M. Preuss, J. W. Thomas, and A. Navarro. 2004. "Chromosomal Rearrangements and the Genomic Distribution of Gene-Expression Divergence in Humans and Chimpanzees." *Trends in Genetics* 20, no. 11: 524–529.

Marshall, C. R., A. Noor, J. B. Vincent, et al. 2008. "Structural Variation of Chromosomes in Autism Spectrum Disorder." *American Journal of Human Genetics* 82, no. 2: 477–488.

McKenna, A., M. Hanna, E. Banks, et al. 2010. "The Genome Analysis Toolkit: A MapReduce Framework for Analyzing Next-Generation DNA Sequencing Data." *Genome Research* 20, no. 9: 1297–1303.

Mérot, C., V. Llaurens, E. Normandeau, L. Bernatchez, and M. Wellenreuther. 2020. "Balancing Selection via Life-History Trade-Offs Maintains an Inversion Polymorphism in a Seaweed Fly." *Nature Communications* 11, no. 1: 670.

Mroczek, R. J., J. R. Melo, A. C. Luce, E. N. Hiatt, and R. K. Dawe. 2006. "The Maize Ab10 Meiotic Drive System Maps to Supernumerary Sequences in a Large Complex Haplotype." *Genetics* 174, no. 1: 145–154.

Muller, H. J. 1930. "Types of Visible Variations Induced by X-Rays in *Drosophila*." *Journal of Genetics* 22: 299–334.

Navarro, A., and N. H. Barton. 2003. "Chromosomal Speciation and Molecular Divergence—Accelerated Evolution in Rearranged Chromosomes." *Science* 300, no. 5617: 321–324.

Navarro, A., E. Betrán, A. Barbadilla, and A. Ruiz. 1997. "Recombination and Gene Flux Caused by Gene Conversion and Crossing Over in Inversion Heterokaryotypes." *Genetics* 146, no. 2: 695–709.

Newman, T. L., E. Tuzun, V. A. Morrison, et al. 2005. "A Genome-Wide Survey of Structural Variation Between Human and Chimpanzee." *Genome Research* 15, no. 10: 1344–1356.

Nosil, P., R. Villoutreix, C. F. de Carvalho, J. L. Feder, T. L. Parchman, and Z. Gompert. 2020. "Ecology Shapes Epistasis in a Genotype-Phenotype-Fitness Map for Stick Insect Colour." *Nature Ecology & Evolution* 4, no. 12: 1673–1684.

O'Donnell, S., and G. Fischer. 2020. "MUM&co: Accurate Detection of all SV Types Through Whole-Genome Alignment." *Bioinformatics* 36, no. 10: 3242–3243.

Olito, C., and J. K. Abbott. 2023. "The Evolution of Suppressed Recombination Between Sex Chromosomes and the Lengths of Evolutionary Strata." *Evolution* 77, no. 4: 1077–1090.

Oneal, E., D. B. Lowry, K. M. Wright, Z. Zhu, and J. H. Willis. 2014. "Divergent Population Structure and Climate Associations of a Chromosomal Inversion Polymorphism Across the *Mimulus Guttatus* Species Complex." *Molecular Ecology* 23, no. 11: 2844–2860.

Ou, S., J. Chen, and N. Jiang. 2018. "Assessing Genome Assembly Quality Using the LTR Assembly Index (LAI)." *Nucleic Acids Research* 46, no. 21: e126.

Pertea, G., and M. Pertea. 2020. "GFF Utilities: GffRead and GffCompare." *F1000Research* 9: 304. https://doi.org/10.12688/f1000research.23297.2.

Pfaffl, M. W. 2001. "A New Mathematical Model for Relative Quantification in Real-Time RT-PCR." *Nucleic Acids Research* 29, no. 9: e45.

Phytozome v13. n.d. Retrieved December 4, 2023. https://phytozome.jgi.doe.gov/info/Mguttatusvar_IM767_v1_1.

Puig, M., S. Casillas, S. Villatoro, and M. Cáceres. 2015. "Human Inversions and Their Functional Consequences." *Briefings in Functional Genomics* 14, no. 5: 369–379.

Pyhäjärvi, T., M. B. Hufford, S. Mezmouk, and J. Ross-Ibarra. 2013. "Complex Patterns of Local Adaptation in Teosinte." *Genome Biology and Evolution* 5, no. 9: 1594–1609.

Qin, M., S. Wu, A. Li, et al. 2019. "LRScaf: Improving Draft Genomes Using Long Noisy Reads." *BMC Genomics* 20, no. 1: 955.

Quinlan, A. R., and I. M. Hall. 2010. "BEDTools: A Flexible Suite of Utilities for Comparing Genomic Features." *Bioinformatics* 26, no. 6: 841–842.

Rane, R. V., L. Rako, M. Kapun, S. F. Lee, and A. A. Hoffmann. 2015. "Genomic Evidence for Role of Inversion 3RP of *Drosophila Melanogaster* in Facilitating Climate Change Adaptation." *Molecular Ecology* 24, no. 10: 2423–2432.

RepeatMasker Home Page. n.d. Retrieved March 13, 2023. http://www.repeatmasker.org/.

Rieseberg, L. H. 2001. "Chromosomal Rearrangements and Speciation." *Trends in Ecology & Evolution* 16, no. 7: 351–358.

Roze, D., and N. H. Barton. 2006. "The Hill–Robertson Effect and the Evolution of Recombination." *Genetics* 173, no. 3: 1793–1811.

Said, I., A. Byrne, V. Serrano, C. Cardeno, C. Vollmers, and R. Corbett-Detig. 2018. "Linked Genetic Variation and Not Genome Structure Causes Widespread Differential Expression Associated With Chromosomal Inversions." *Proceedings of the National Academy of Sciences of the United States of America* 115, no. 21: 5492–5497.

Schaefer, H. M., and G. Rolshausen. 2006. "Plants on Red Alert: Do Insects Pay Attention?" *BioEssays: News and Reviews in Molecular, Cellular and Developmental Biology* 28, no. 1: 65–71.

Schneider, M., A. Bairoch, C. H. Wu, and R. Apweiler. 2005. "Plant Protein Annotation in the UniProt Knowledgebase." *Plant Physiology* 138, no. 1: 59–66.

Schwander, T., R. Libbrecht, and L. Keller. 2014. "Supergenes and Complex Phenotypes." *Current Biology* 24, no. 7: R288–R294.

Shumate, A., and S. L. Salzberg. 2020. "Liftoff: Accurate Mapping of Gene Annotations." *Bioinformatics* 37, no. 12: 1639–1643.

Simão, F. A., R. M. Waterhouse, P. Ioannidis, E. V. Kriventseva, and E. M. Zdobnov. 2015. "BUSCO: Assessing Genome Assembly and Annotation Completeness With Single-Copy Orthologs." *Bioinformatics* 31, no. 19: 3210–3212.

Slater, G. S. C., and E. Birney. 2005. "Automated Generation of Heuristics for Biological Sequence Comparison." *BMC Bioinformatics* 6: 31.

Stanke, M., and B. Morgenstern. 2005. "Augustus: A Web Server for Gene Prediction in Eukaryotes That Allows User-Defined Constraints." *Nucleic Acids Research* 33: W465–W467.

Tang, H., X. Zhang, C. Miao, et al. 2015. "ALLMAPS: Robust Scaffold Ordering Based on Multiple Maps." *Genome Biology* 16, no. 1: 3.

Thompson, M. J., and C. D. Jiggins. 2014. "Supergenes and Their Role in Evolution." *Heredity* 113, no. 1: 1–8.

Todesco, M., G. L. Owens, N. Bercovich, et al. 2020. "Massive Haplotypes Underlie Ecotypic Differentiation in Sunflowers." *Nature* 584, no. 7822: 602–607.

Tuttle, E. M., A. O. Bergland, M. L. Korody, et al. 2016. "Divergence and Functional Degradation of a Sex Chromosome-Like Supergene." *Current Biology* 26, no. 3: 344–350.

Twyford, A. D., and J. Friedman. 2015. "Adaptive Divergence in the Monkey Flower *Mimulus guttatus* Is Maintained by a Chromosomal Inversion." *Evolution* 69, no. 6: 1476–1486.

Vaser, R., I. Sović, N. Nagarajan, and M. Šikić. 2017. "Fast and Accurate de Novo Genome Assembly From Long Uncorrected Reads." *Genome Research* 27, no. 5: 737–746.

Vasimuddin, M., S. Misra, H. Li, and S. Aluru. 2019. "Efficient Architecture-Aware Acceleration of BWA-MEM for Multicore Systems." *2019 IEEE International Parallel and Distributed Processing Symposium*: 314–324.

Veltsos, P., L. J. Madrigal-Roca, and J. K. Kelly. 2024. "Testing the Evolutionary Theory of Inversion Polymorphisms in the Yellow Monkeyflower (*Mimulus guttatus*)." *Nature Communications* 15, no. 1: 10397.

Villoutreix, R., D. Ayala, M. Joron, Z. Gompert, J. L. Feder, and P. Nosil. 2021. "Inversion Breakpoints and the Evolution of Supergenes." *Molecular Ecology* 30, no. 12: 2738–2755.

Vogel, M. J., L. Pagie, W. Talhout, M. Nieuwland, R. M. Kerkhoven, and B. van Steensel. 2009. "High-Resolution Mapping of Heterochromatin Redistribution in a *Drosophila* Position-Effect Variegation Model." *Epigenetics & Chromatin* 2, no. 1: 1.

Walker, B. J., T. Abeel, T. Shea, et al. 2014. "Pilon: An Integrated Tool for Comprehensive Microbial Variant Detection and Genome Assembly Improvement." *PLoS One* 9, no. 11: e112963.

Wang, K., M. Li, and H. Hakonarson. 2010. "ANNOVAR: Functional Annotation of Genetic Variants From High-Throughput Sequencing Data." *Nucleic Acids Research* 38, no. 16: e164.

Wong, E. L. Y., and D. A. Filatov. 2023. "The Role of Recombination Landscape in Species Hybridisation and Speciation." *Frontiers in Plant Science* 14: 1223148.

Zhang, Z., H. Zhu, B. S. Gill, and W. Li. 2015. "Fine Mapping of Shattering Locus Br2 Reveals a Putative Chromosomal Inversion Polymorphism Between the Two Lineages of *Aegilops tauschii*." *Theoretical and Applied Genetics* 128, no. 4: 745–755.

Zhou, H., R. Ma, L. Gao, et al. 2021. "A 1.7-Mb Chromosomal Inversion Downstream of a PpOFP1 Gene Is Responsible for Flat Fruit Shape in Peach." *Plant Biotechnology Journal* 19, no. 1: 192–205.

Supporting Information

Additional supporting information can be found online in the Supporting Information section.